



HAL
open science

Combined impact of selected material properties and environmental conditions on the swelling pressure of compacted claystone/bentonite mixtures

Marvin Middelhoff, O. Cuisinier, F. Masrouri, J. Talandier, N. Conil

► To cite this version:

Marvin Middelhoff, O. Cuisinier, F. Masrouri, J. Talandier, N. Conil. Combined impact of selected material properties and environmental conditions on the swelling pressure of compacted claystone/bentonite mixtures. *Applied Clay Science*, 2019, 184, pp.105389. 10.1016/j.clay.2019.105389 . hal-02420205

HAL Id: hal-02420205

<https://hal.univ-lorraine.fr/hal-02420205>

Submitted on 21 Jul 2022

HAL is a multi-disciplinary open access archive for the deposit and dissemination of scientific research documents, whether they are published or not. The documents may come from teaching and research institutions in France or abroad, or from public or private research centers.

L'archive ouverte pluridisciplinaire **HAL**, est destinée au dépôt et à la diffusion de documents scientifiques de niveau recherche, publiés ou non, émanant des établissements d'enseignement et de recherche français ou étrangers, des laboratoires publics ou privés.



Distributed under a Creative Commons Attribution - NonCommercial 4.0 International License

1 **Combined impact of selected material properties and environmental condi-** 2 **tions on the swelling pressure of compacted claystone/ bentonite mixtures**

3 M. Middelhoff ^{1,2*}, O. Cuisinier ¹, F. Masrouri ¹, J. Talandier ², N. Conil ²

4 ¹ Université de Lorraine – LEMTA, UMR 7563 CNRS,
5 (2 Rue du Doyen Marcel Roubault - BP 10162, 54505 Vandœuvre-lès-Nancy CEDEX, France)

6 ² Agence nationale pour la gestion des déchets radioactifs (ANDRA), France

7 Marvin.Middelhoff@univ-lorraine.fr

8 Abstract: Mixtures composed of 70% crushed Callovo-Oxfordian claystone and 30% MX80-bentonite
9 are considered as materials, that could be used for backfilling a future radioactive waste repository in
10 deep sedimentary rock formations. Their characterization is of interest, as the replacement of fractions
11 of crushed claystone by bentonite enhances the chemo-hydro-mechanical performance of backfill. The
12 materials are envisaged to be installed directly in the drifts and shafts by means of conventional com-
13 paction techniques. The hydro-mechanical behavior of materials containing expansive mineral phases,
14 and especially their swelling behavior, is known to be significantly affected by the initial material prop-
15 erties and environmental and stress conditions. The present study aimed to assess the combined impact
16 of variations in the material properties and environmental conditions, particularly the grain size distri-
17 bution, dry density and saturating solution chemistry, on the swelling pressure of the mixtures, by con-
18 ducting a comprehensive laboratory experimental program. The results revealed that the adjustment of
19 the grain size distribution of employed bentonite enhanced the compaction behavior and, in turn, the
20 swelling behavior of the mixtures. Generally, swelling pressures of mixtures were less affected by the
21 employed saline and alkaline solutions than those of crushed claystone. The measured swelling pres-
22 sures were exponentially related to the initial dry density of the expansive mineral phase, regardless of
23 the grain size distribution. Based upon the finding that the expansive mineral phase being present in
24 crushed claystone contributed to measured swelling pressures, a new approach was introduced to calcu-
25 late the dry density of the expansive mineral phase in bentonites and their mixtures with non-expansive
26 or less-expansive materials.

27 Keywords: Callovo-Oxfordian claystone, MX80-bentonite, Swelling pressure, Grain-size distribution,
28 Dry density, Solution chemistry

29 Highlights:

- 30 • Grain size distribution of bentonite influenced material performance of the mixtures
- 31 • Adjusting the grain size distribution of bentonite increased the highest swelling pressure
- 32 • Solution chemistry had little impact on the short-term evolution of the swelling pressure
- 33 • Impact of expansive minerals in claystone on the swelling pressure was considered

34 1 Introduction

35 The long-term integrity of geological repository systems for nuclear waste is envisaged
36 to be ensured by means of installing a multiple barrier system, which is generally composed of
37 waste canisters, backfill, seals and the surrounding geological formation. The major contain-
38 ment might be either the geological formation or the canister, depending on the disposal con-
39 cept.

40 According to Andra (2005), the French concept favors the former. It plans to install the
41 future repository for disposing intermediate and high-level waste (ILW/ HLW) in the clay-rich
42 Callovo-Oxfordian (COX) sedimentary rock formation, henceforth referred to as COX-clay-
43 stone. Since the construction of drifts and shafts reduces the integrity of the geological for-
44 mation, backfill and seals serve the general purpose of recovering the integrity upon terminating
45 the closure-phase. Both are envisaged to fill hydraulic conductive voids and to limit the propa-
46 gation of the excavation-damaged zone (EDZ) by stabilizing the surrounding rock mass. In
47 addition, seals compress the EDZ, and fluxes of fluid phases from the repository to the bio-
48 sphere and vice versa are inhibited by these means. Based on the mentioned purposes, the po-
49 tential seal and backfill materials must exhibit a swelling potential, as well as strength. Specif-
50 ically, the seal material must possess hydraulic conductivity, which ensures the inhibition of
51 fluid fluxes. Andra (2005) proposed the employment of bentonite as a pure material or as a
52 dominant fraction of a mixture with non- or less-expansive material, such as sand or crushed
53 COX-claystone (COX_c), to seal the drifts and shafts. Conversely, backfill material consists of
54 COX_c, which can be alternatively mixed with minor fractions of bentonite. The re-employment
55 pursues the objectives of reducing the negative impact of backfill on the surrounding geological
56 formation, avoiding mineralogical and physico-chemical incompatibilities, and lowering the
57 costs by replacing commercial bentonite with COX_c. Determined in a manifold fashion, the
58 hydro-mechanical behavior of materials containing expansive mineral phases is significantly

59 affected by the material properties, the stress history and the environmental conditions (Chen,
60 1988; Gens and Alonso, 1992).

61 Different techniques have been considered to install backfill and seals. Seals are con-
62 structed by emplacing either industrially fabricated blocks or pellets into the drifts and shafts.
63 Their industrial fabrication offsite is advantageous, since the initial dry density can be adapted
64 to the target values by using, for instance, the required compaction energy. Conversely, the
65 employment of conventional techniques, such as vibrating plates, is envisaged to compact back-
66 fill layer wise in situ. As the applicable compaction energy is limited in the case of in situ
67 compaction, the initial dry density varies as a function of the initial water content. Generally,
68 the maximum dry density is attained at the optimum water content by using constant compac-
69 tion energy. The backfill is characterized by a lower initial dry density and a significantly higher
70 water content, compared to blocks and pellets (Andra, 2005).

71 The feasibility of in situ compaction as a potential technique for backfill installation was
72 evaluated by Gunnarson et al. (2001) and Johannesson (2014). They aimed to compact the
73 backfill to the maximum dry density at the optimum water content, since the highest swelling
74 pressure and low hydraulic conductivity are likely to be attained by this means (Mitchell and
75 Soga, 2005). It was hardly realizable to homogeneously compact the material in the cross-sec-
76 tion of the drift, especially close to the drift top and walls. They referred to the issues of the
77 position of the compactor, which caused a loss of compaction energy and, in turn, a reduction
78 in the initial dry density up to 20% with respect to the maximum dry density. Great differences
79 in the swelling pressures were thus attributed to variations in these material properties.

80 In addition to varying material properties, evolving environmental conditions, such as
81 saturating solution chemistry, are likely to have a negative impact on the performance of back-
82 fill materials containing expansive mineral phases. The phenomenon known as alkaline plume
83 triggers the dissolution and modification of clay minerals in the backfill material, altering its

84 structure and, in turn, its performance (Bradbury and Baeyens, 2003; Pusch et al., 2003;
85 Karnland et al., 2007; Cuisinier et al., 2009; Cuisinier et al., 2014) These combined variations
86 in the material properties and environmental conditions can impair the performance of backfill
87 materials in such a way that formulated safety requirements are not met.

88 As information about COX_c was limited, most studies performed within the last few years
89 were focused on characterizing the volume change and hydraulic conductivity behavior, rather
90 than considering additional variations in material properties and environmental conditions.

91 Tang et al. (2010), Tang et al. (2011a) and Tang et al. (2011b) compacted COX_c to initial
92 dry densities of $\approx 2 \text{ Mg/m}^3$ at water contents of $\approx 3 \%$. These densities were in accordance with
93 the envisaged densities of blocks being employed for seal construction. The obtained results
94 indicated that the swelling pressures ranged from several hundreds of kPa to some MPa. The
95 measured hydraulic conductivities were equal to those of intact drill cores of COX. Wang et al.
96 (2012) and Wang et al. (2014) performed swelling pressure and free swell experiments on com-
97 pacted MX80-bentonite/ COX_c-mixtures, which were predominantly composed of MX80-ben-
98 tonite ($\approx 70\%$). Their experiments considered not only a variety of soil properties and environ-
99 mental conditions but also time effects. Just like in the sand-bentonite mixtures, the magnitude
100 of material swelling was exponentially related to the initial dry density and was hardly affected
101 by the saturation with a solution of low ionic strength. It can be concluded that few studies have
102 examined mixtures of materials that each contains expansive mineral phases. Moreover, the
103 performed experimental programs have hardly considered the variations in the initial material
104 properties, as well as environmental conditions and their impact on the hydro-mechanical be-
105 havior of these mixtures.

106 This experimental program assessed the impact of replacing 30% of COX_c with MX80-
107 bentonite on the structure, as well as the impacts on the compaction characteristics and on the
108 swelling pressure. In particular, the consideration of the total amount of expansive mineral

109 phases in these mixtures was of major interest, as the expansive mineral phases in COX_c were
110 expected to contribute to the evolution of the swelling pressure. Bentonite was processed to
111 maximum grain sizes of 0.25 mm and 2.00 mm before being mixed with COX_c. Henceforth,
112 the mixtures of COX_c with bentonite with maximum grain sizes of 0.25 mm and 2.00 mm are
113 referred to as the powder mixture and the grain mixture, respectively. The short-term develop-
114 ment of the swelling pressure was tested by adopting the constant-volume method. Based on
115 the findings of Gunnarson et al. (2001), the impact of varying the dry densities on the short-
116 term evolution of the swelling pressure was investigated by compacting the mixtures to their
117 maximum and reduced dry densities at the optimum water content. The complementing exper-
118 iments aimed to assess the impact of solutions with different pH values and ionic strengths on
119 samples that were compacted to their maximum dry density at the optimum water content.
120 Eventually, their combined impact on the performance of claystone/ bentonite-mixtures was
121 analyzed in terms of the swelling pressure.

122 2 Theoretical Background

123 The impact of variations in the saturating solution chemistry and dry density on the swell-
124 ing behavior of claystone/ bentonite-mixtures is predominantly related to the physico-chemical
125 forces at the molecular scale, namely, attractive and repulsive forces, that occur when saturating
126 expansive clay minerals. These forces, in turn, are affected by the structure of the mixtures
127 (Mitchell and Soga, 2005).

128 The mineralogical composition of MX80-bentonite is dominated by montmorillonite
129 (Müller-Vonmoos and Kahr, 1983; Herbert et al., 2004; Karnland et al., 2007). Table 1 com-
130 piles information about the mineralogical composition of MX80-bentonite taken from the liter-
131 ature. Single montmorillonite particles are characterized by both their platy form and their var-
132 iable thickness. Their unit layers are composed of one alumina sheet that is sandwiched between
133 two silica sheets. The permanently negative surface charge at their basal planes is attributable

134 to isomorphous substitution, which is usually compensated by exchangeable cations, while the
135 surface charges at their edge faces vary as a function of the proton concentration in the solution.
136 Positively charged species are thus attracted by basal planes and either attracted or repelled by
137 the edge faces (van Olphen, 1977; Tombácz and Szekeres, 2004, 2006). Regardless of the sur-
138 face charge, dissolution and modification processes alter the clay minerals and their structures,
139 in cases where they are exposed to solutions of different pH (Bradbury and Baeyens, 2003).
140 These processes account for the sensitivity of expansive clays to varying pH values.

141 Apart from the pH, the swelling behavior of expansive clays is also affected by the ionic
142 strength of the solution. Once montmorillonite particles are saturated with aqueous solution,
143 the cations and water molecules are adsorbed by attractive forces on particle surfaces, forming
144 diffuse double layers. Water molecules additionally permeate the interlayer space due to the
145 higher hydration potential (Yong, 1999; Pusch and Yong, 2003). The concentration of the cat-
146 ions is high close to the particle surface and declines exponentially, as the distance from the
147 particle surface increases. Repulsive forces occur once the diffuse double layers of the neigh-
148 boring particles overlap (Bolt, 1956; Sridharan et al., 1986; Mitchell and Soga, 2005). Among
149 other factors, the thickness of the diffuse double layers varies as a function of the ion concen-
150 tration and ionic strength (Mitchell and Soga, 2005).

151 Swelling itself is comprised of two processes, namely, crystalline and osmotic swelling,
152 occurring upon hydration of expansive clay particles (Madsen and Müller-Vonmoos, 1989).
153 Among other factors, such as the interlayer cation nature, their magnitude is related to the pH
154 and ionic strength of the solution. Crystalline swelling is the result of the progressive hydration
155 of exchangeable cations in the interlayer space, while osmotic swelling is caused by the inter-
156 action of overlapping diffuse double layers formed on neighboring clay particles. More detailed
157 information about clay swelling is given in Madsen and Müller-Vonmoos (1989), Sridharan
158 and Choudhury (2002) and Schanz and Tripathy (2009). Swelling pressure can be considered

159 as the sum of hydration and repulsion forces, that accumulate upon saturation of expansive
160 clays under confined conditions. Conversely, free swell strains develop under free conditions
161 (Madsen and Müller-Vonmoos, 1989).

162 Attractive and repulsive forces account for the structure of the compacted expansive clays
163 at the micro- and macro-scales. However, their structure is hardly affected by the ionic strength
164 and pH of the adjacent solution. Generally, multiple clay particles form aggregates at the micro-
165 scale, in which the single particles are orientated predominantly parallel due to the repulsion of
166 equally charged particle faces. The random assembly of multiple aggregates constitutes macro-
167 scale structures. Several studies, such as those of Alonso et al. (1987), Lloret et al. (2003) and
168 Delage et al. (2006), analyzed the pore size distribution in expansive clays compacted by fol-
169 lowing the approach of block fabrication. Their results showed, that the total pore space is com-
170 prised of different kinds of pore populations at different scales, being characterized by a bi-
171 modal-shaped pore size distribution curve. Interlayer spaces are planar void spaces between the
172 unit layers, while the inter-particle pores are present between particles and inside aggregates.
173 Randomly arranged aggregates account for the inter-aggregate pores. The latter two pore pop-
174 ulations are referred to as micro-pores and macro-pores. Increasing dry densities cause a sig-
175 nificant reduction in the macro-porosity, while the micro-porosity remains stable. Overlapping
176 repulsive forces contribute to the conservation of micro-porosity (Lloret et al., 2003).

177 The exponential relation of the initial dry density and the maximum values of the swelling
178 pressure and free swell strains were determined in several studies (Komine et al., 2009; Schanz
179 and Tripathy, 2009; Baille et al., 2010). The mentioned literature elaborately informs about the
180 approaches adopted to explain this exponential relation.

181 This experimental program quantified the enhancement of the swelling behavior attainable
182 by mixing COX_c with bentonite. The obtained results were complemented by information

183 regarding the contribution of expansive mineral phases in COX_c to the maximum swelling pres-
184 sure of mixtures. Moreover, the experiments aimed to determine, whether the swelling behavior
185 of COX_c and its mixtures is more susceptible to variations in initial dry density or saturating
186 solution chemistry, since information about their impact is scarcely available. A comprehensive
187 platform was provided by these means, permitting to assign the observations to the single and
188 combined impacts.

189 3 Materials

190 COX-claystone was obtained by excavating drifts of ANDRA URL in Bure at a depth of
191 – 490 m. A few weeks afterwards, the excavated material was industrially crushed to maximum
192 grain sizes of 2.00 mm and filled into sealed barrels. According to Robinet et al. (2012) and
193 Conil et al. (2018), the mineralogical composition, initial water content and initial porosity of
194 COX-claystone vary depending on the location in the sedimentary layer. COX-claystone is
195 composed of 20 – 60% clay minerals being dominated by illite and interstratified illite/ smec-
196 tite, 10 – 40% quartz and feldspars, 15 – 80% carbonates, and low amounts of pyrites. In con-
197 trast to intact drill cores of COX-claystone, whose initial water content are approximately 8.0%
198 (Conil et al., 2018), the water content of COX_c was 5.4%. This decrease was attributed to the
199 crushing process and the duration of the storage. MX80-bentonite (Wyoming, USA) was se-
200 lected to be mixed with COX_c, since it exhibits beneficial material properties, especially re-
201 garding its high volume change, low conductivity and high retention behavior (Pusch, 1992).
202 Like COX_c, it was industrially crushed to maximum grain diameters of 0.28 mm and 2.00 mm,
203 and filled by the supplier (Laviosa-MPC SAS, Limay, France) into sealed buckets. Information
204 regarding the approximated mineralogical composition of the employed MX80-bentonite is
205 given in Table 1. The water content, liquid limit, plastic limit and specific gravity of COX_c and

206 the mixtures were determined following the French standard (AFNOR, 1991, 1993). The deter-
207 mined physical properties of COX_c and the mixtures are compiled in Table 2. The correspond-
208 ing values of MX80-bentonite are provided for the purpose of comparison.

209 The grain size distribution curves were obtained in two steps. First, grains larger than
210 0.80 mm in diameter were separated from the finer fractions via dry sieving. Since the bentonite
211 fraction in the mixtures was expected to clog the finer meshes when coming into contact with
212 water, the method of dry sieving was favored over wet sieving. The grain size distribution of
213 the finer fractions was measured via laser diffractometry, following ISO (2009). The obtained
214 distribution curves are depicted in Figure 1. The replacement of COX_c by bentonite with a
215 maximum grain size of 0.28 mm caused a shift in the distribution curve to higher values, cor-
216 responding to a general increase in the amount of fines in the powder mixture.

217 Sample preparation, as well as standard and modified Proctor tests, were conducted ac-
218 cording to the French standard (AFNOR, 2014). The materials were prepared in a mechanical
219 mixer at various molding water contents and filled in plastic bags after termination of the mix-
220 ing process. Various molding water contents were established by adding deaired/ demineralized
221 water to the original materials. The bags were then stored under ambient room conditions ($T =$
222 $20 \pm 2^\circ\text{C}$). During a period of one week, the plastic bags were frequently revolved to guarantee
223 a homogeneous water content distribution. The results of the standard and modified Proctors
224 tests performed on COX_c and the mixtures are depicted in Figure 2 a and b. The replacement of
225 COX_c reduced the maximum dry density considerably and shifted the optimum water contents
226 to higher values, regardless of the applied compaction energy. In the case of compacting the
227 mixtures by using standard compaction energy, the impact of an increasing water content on
228 the dry density at the dry side of the optimum water content was negligible.

229 Three different aqueous solutions, namely, deionized/ demineralized water (DW), artifi-
230 cial Bure site solution (ABSS) and artificial Portland cement solution (APCS), were employed.

231 They varied in their chemical compositions, ionic strengths and pH values. DW represented the
232 reference case, since its chemical composition was expected to not affect the material behavior,
233 while ABSS and APCS were believed to alter the swelling behavior as the site water at a depth
234 of – 490 m and the occurring hyperalkaline solution, respectively. Both solutions were prepared
235 according to information given by ANDRA. The compounds, main ion species and other char-
236 acteristics of ABSS and APCS are compiled in Table 3.

237 4 Methods

238 The materials were prepared following the previously established protocol (Section 3).
239 The samples were envisaged to be compacted to maximum dry densities ($\pm 1\%$) at individual
240 optimum water contents ($\pm 1\%$), as determined in modified Proctor tests. Variations in the
241 initial dry density were portrayed by reducing the maximum dry density of samples by 2.5%,
242 7.5% and 17.5%, while keeping the optimum water content. In the following, coefficients of
243 dry density reduction were indicated by $R_{pd, max}$. Although it must be assumed that values of the
244 initial dry density were shifted to the dry side of the compaction curve by reducing the maxi-
245 mum dry density and keeping the optimum water content, the approach was believed to ade-
246 quately portray the conditions in situ. The reduction of the initial dry density by 17.5% with
247 respect to the maximum dry density, for instance, corresponds to a loss of compaction energy
248 of approximately 20%. Such a loss of compaction energy is likely to occur, if the materials are
249 compacted close to the drift wall or the drift top. Conversely, the preparation of backfill mate-
250 rials to their optimum water contents and their conservation were less challenging tasks in situ
251 (Gunnarson et al., 2001).

252 The samples were compacted statically to target dry densities at a controlled rate of
253 0.1 mm/s inside the rings. The initial dimensions of each sample were 15 mm in height and
254 70 mm in diameter. By compacting the samples directly inside the rings, the risk of creating

255 preferential flow paths and, in turn, saturating the samples heterogeneously, was significantly
256 reduced. The ring, which contained the compacted sample being sandwiched between two po-
257 rous discs, was screwed to the lid and the bottom plate. Then, the assembled cell was positioned
258 in a load frame and the bottom plate was connected to a volume-/ pressure control unit, enabling
259 the saturation of the sample with a given pressure from the bottom of the cell upwards. A grad-
260 uated flask was used to collect the outflowing solution. The load frame was equipped with an
261 external load sensor, an internal load sensor, and a linear transducer. The linear transducer mon-
262 itored the vertical position of the piston. Detecting an upward movement that was triggered by
263 material swelling, the load frame automatically adapted the position of the piston downwards.
264 By these means, the volume was kept constant. The evolving swelling pressure was recorded
265 by two load sensors.

266 First, the experiment protocol envisaged to subject the samples to a vertical stress equal
267 to 10 kPa. This approach served the purpose of establishing a good contact between the bottom
268 plate, the porous disks, the sample, and the piston. The load frame kept the position of the piston
269 constant afterwards. The bottom plate was flushed before imposing the injection pressure of
270 15 kPa, corresponding to a hydraulic gradient of 100, considering a sample height of 15 mm.
271 By these means, the residual air in the bottom plate was removed. The swelling pressure exper-
272 iments were stopped after 10 000 minutes (≈ 7 days). Detailed information about the samples
273 and their major initial characteristics are given in the first part of the supplementary materials.

274 5 Results

275 The constant-volume swelling pressure experiments aimed to investigate the impact of
276 replacing 30% of COX_c with bentonite on the short-term evolution of the swelling pressure of
277 COX_c and the mixtures. The complementing experiments analyzed the response of the swelling
278 pressure to variations in the dry density, as well as the saturating solution chemistry.

279 The evolutions of the swelling pressure of COX_c and the mixtures are depicted in Fig-
280 ure 3. Materials being compacted using higher energies generally exhibited higher swelling
281 pressures. The maximum swelling pressures of COX_c and the grain-mixture were comparably
282 low, while the powder-mixture was characterized by slightly elevated pressures, if it was com-
283 pacted using standard energy. The maximum swelling pressure of the powder-mixture was
284 990 kPa, corresponding to an increase by 30% and 65%, compared to the maximum values of
285 the grain-mixture and COX_c, respectively.

286 Generally identified, the mixtures reacted to variations in solution chemistry less suscep-
287 tibly than COX_c, when being compacted to maximum dry densities at optimum water contents.
288 The impact of variations in the solution chemistry was thus more pronounced in the case of
289 COX_c. The comparison of the material response is depicted in Figure 4. It became evident that
290 the alkaline solution impaired the material performance more significantly than ABSS, alt-
291 hough it had a lower ionic strength. For instance, the saturation with ABSS reduced the maxi-
292 mum swelling pressure by 6% in the case of the grain mixture and by 44% in case of COX_c.
293 The grain-mixture lost 13% of its maximum swelling pressure, while a loss of 69% was meas-
294 ured upon bringing COX_c in contact with APCS.

295 The reduction in the dry density caused a significant loss in the swelling pressure in the
296 individual experiments, when compacting the material at optimum water content. The impact
297 of the reduced dry densities in the case of the grain-mixture is presented in Figure 5. Accord-
298 ingly, maximum values were determined at the highest dry densities. A reduction of 2.5%, 7.5%
299 and 17.5% decreased the maximum swelling pressure by 20%, 65% and 85%, respectively.
300 Moreover, the material saturation accelerated as the dry density decreased. The reduction in the
301 maximum dry density and the maximum swelling pressure of both mixtures were exponentially
302 related (Figure 6 a and b). The corresponding regression line is given by the equation:

$$\sigma_s = \sigma_{s,max} \exp(-\beta R_{\rho_d,max}) \quad (5.1)$$

303 where $\sigma_{s, max}$ is the highest expectable swelling pressure and β is the slope indicating the
304 swelling pressure decrease with the dry density reduction. As already identified, even a reduc-
305 tion in the material dry density of 2.5% provoked a significant decrease of swelling pressure,
306 regardless of the mixture and the saturating solution chemistry. The values of the β -parameters
307 of grain- and powder-mixtures were in the same range, indicating a similar impact of the solu-
308 tion chemistry on the short-term material performance. However, the values were smaller com-
309 pared to the others, in the case of the β -parameters of ABSS.

310 The major results of the performed swelling pressure experiments are compiled in the
311 second part of the supplementary materials. Information about the major final characteristics of
312 samples are added. The expansive mineral dry density (EDD) will be introduced in section 6.1.

313 6 Discussion

314 Most of obtained results are neither comparable nor interpretable with relations that are
315 presented in the literature, since the reduction in the maximum dry density $R_{pd, max}$ represents a
316 value being relative to the individual maximum dry density. Thus, replacing the reduction by a
317 generally more applicable variable might be recommended. Section 6.1 briefly introduces the
318 expansive material dry density (EDD) and its major purpose, while the following sections dis-
319 cuss the obtained results.

320 6.1 Introduction of expansive mineral dry density (EDD)

321 COX_c and MX80-bentonite are referred to as expansive materials that are generally com-
322 posed of expansive and inert mineral phases. Results of constant-volume swelling pressure ex-
323 periments performed on COX_c suggested a non-negligible contribution of the expansive mineral
324 phases in COX_c to the maximum swelling pressure of mixtures (Figure 3). It was thus assumed
325 that the total fraction of the expansive mineral phases must account for the swelling character-

326 istics of mixtures. Concepts such as the bentonite dry density attributing the behavior of mix-
327 tures of bentonite and non-expansive materials only to the bentonite fraction (Bucher and Jedel-
328 hauser, 1985; Villar and Rivas, 1994; Dixon, 2000; Agus and Schanz, 2008; Wang et al., 2012)
329 were hardly applicable in the case of claystone/ bentonite mixtures, as they disregard expansive
330 mineral phases in COX_c on the one hand and inert mineral phases in MX80-bentonite on the
331 other hand. Unlike the approach of Zeng et al. (2019) which considered the contribution of
332 expansive mineral phases in COX_c to material swelling of bentonite/ claystone mixtures by
333 introducing an inhibition factor, the expansive mineral dry density (EDD) was aimed at relating
334 the swelling characteristics of bentonites and their mixtures to their mineralogical composition.
335 Apart from attributing material swelling to the total fraction of the expansive mineral phases in
336 the mixtures, the following assumptions are also considered prior to its employment. The pore
337 water being present is exclusively attached to the expansive mineral phases; the porosity of the
338 fraction of inert mineral phases is so low that expansive mineral phases occupy the entire macro-
339 pore space when they swell; and material compaction only causes a reduction in the macro-pore
340 space.

341 In the following, materials containing expansive mineral phases are classified into the
342 expansive and inert mineral phases, as well as the fluid phase and the gas phase. The corre-
343 sponding phase diagram is depicted in Figure 7. The total fraction of expansive mineral phases
344 in the mixtures was calculated by first summing the fraction of expansive mineral phases (x_{ji})
345 in each material (i) up and then multiplying the obtained sum by the total fraction of the corre-
346 sponding material in the mixture (f_i). The results of the second step were then summarized to
347 consider all materials in the mixture. The total fraction of inert mineral phases in the mixtures
348 was calculated similarly. For instance, the total fraction of smectite in the mixture was calcu-
349 lated by first multiplying 0.83 (Table 1) representing the fraction of smectite in MX80-bentonite
350 by 0.3 representing the fraction of MX80-bentonite in the mixture. The fraction of smectite in

351 COX_c was assumed to be equal to 0.15 as COX_c only contains fractions of interstratified il-
 352 lite/smectite. Its multiplication by 0.7 makes the fraction of smectite in COX_c. The final value
 353 of the fraction of smectite in the mixture is obtained by summing 0.25 and 0.15 up being equal
 354 to 0.35. EDD was defined as the ratio of the dry mass of the total fraction of expansive mineral
 355 phases in the mixture to the combined volume of the total fraction of expansive mineral phases
 356 in the mixture and the pore volume. The denominator of the ratio is substitutable by the differ-
 357 ence between the total volume of the mixture and the volume of the total fraction of inert min-
 358 eral phases in the mixture. EDD is given as:

$$EDD = \left[\sum_i \sum_j f_i x_{ji} \right] \left[\frac{1}{\rho_d} - \left(\frac{1 + w_{ini}}{\rho_w} \right) \left[\sum_i \sum_k \frac{f_i y_{ki}}{G_{s\ ki}} \right] \right]^{-1} \quad (6.1)$$

359 where f_i is the mass fraction of material i in the mixture, x_{ji} is the mass fraction of expan-
 360 sive mineral phase j in material i , y_{ki} is the mass fraction of inert mineral phase k in material i
 361 and $G_{s\ ki}$ is the specific gravity of the inert mineral phase k in the material i . For instance, the
 362 calculation of the mass fraction of smectite in the investigated mixtures proceeds as follows:
 363 The mass fraction of MX80-bentonite in the mixture is initially multiplied by the mass fraction
 364 of smectite in MX80-bentonite. Similarly, the mass fraction of smectite in COX_c, which is pre-
 365 sent in the mixture, is calculated in the next step. The sum of both multiplications eventually
 366 gives the mass fraction of smectite in the investigated mixtures.

367 The equation is complemented by the dry density of the mixture (ρ_d), the density of the
 368 water (ρ_w), and the initial water content of the mixture (w_{ini}). Its utilization allowed a compari-
 369 son of the impact of densification on the maximum swelling pressure of not only the bentonites
 370 being predominantly composed of expansive minerals, such as MX80-bentonite, but also mix-
 371 tures of those bentonites with less- and non-expansive materials, such as COX_c or sand.

372 6.2 Impact of expansive mineral content and grain size distribution

373 First, the impact of COX_c-replacement by bentonite on the compaction and swelling prop-
374 erties was assessed. Comparing the compaction curves of COX_c and both mixtures, COX_c ex-
375 hibited a significantly higher compactibility, indicated by the higher dry densities (Figure 2).
376 The compaction behavior of the mixtures was alike that of pure MX80-bentonite, since varying
377 water contents had a minor impact on the attained dry densities at the dry side of the compaction
378 curve (Dixon et al., 1985). These findings were complemented by Pusch (1995), Keto et al.
379 (2006) and this study. They observed a more pronounced sensitivity of material dry density to
380 varying water content and compaction energy with a lower amount of expansive material in the
381 mixture. Dixon et al. (1985) related the observed insensitivity of MX80-bentonite to the higher
382 viscosity of adsorbed water on clay particles, which induces an elevated shear strength. This
383 resistance might be higher than the applied compaction energies. Consequently, the shear
384 strength might decrease with an increasing amount of less- or non-expansive material. As de-
385 scribed by Komine and Ogata (1999), an increasing fraction of expansive material in these
386 mixtures provokes higher swelling pressures, if compacted to maximum dry density at optimum
387 water content.

388 Referring to the impact of the amount of fines on the compaction and swelling properties,
389 it became evident that the powder-mixture exhibited a higher compactability than the grain-
390 mixture when compacting it by using the modified compaction energy. The measured swelling
391 pressures of the powder-mixture were higher than those of the grain-mixture due to the higher
392 dry density and the lower optimum water content. Keto et al. (2006) performed modified Proc-
393 tor experiments on crushed granite rock/ bentonite-mixtures. According to their findings, the
394 highest dry densities can be attained by employing materials having the widest grain size dis-
395 tribution and the highest amount of fines. A wider grain size distribution provokes a denser
396 packing of particles and, in turn, reduces the amount of macro-porosity.

397 6.3 Individual impact of EDD and solution chemistry

398 The introduction of EDD aimed to compare the impact of densification on any material
399 that contains fractions of expansive minerals. Its applicability was verified by calculating EDD
400 derived from different literature and plotting the values against the reported maximum swelling
401 pressures. The obtained results compared to the literature data are depicted in Figure 8. The
402 comparison affirmed the significance of EDD as one key variable governing the maximum
403 swelling pressure of materials containing expansive mineral phases. The grain- and powder-
404 mixtures reacted to elevated EDD with increasing swelling pressures as depicted in Figure 8.
405 According to section 2, these results were most likely attributable to the higher probability of
406 double layer repulsion. The exponential relationship of EDD and the maximum swelling pres-
407 sure of each bentonite, including its mixtures, seemed to be unique although this issue has not
408 been confirmed. This trend was particularly noticeable by comparing the slope of the individual
409 regression lines of the materials composed of MX80-bentonite. The general trend can be ap-
410 proximated by the following generalized equation of the regression curve:

$$\sigma_{s,max} = \sigma_{s,min} \exp(\beta^* EDD) \quad (6.2)$$

411 where $\sigma_{s, min}$ can be considered to be the minimal swelling pressure that is theoretically
412 evolving, if the material is in a loose state, while β^* identifies the actual impact of varying EDD
413 on the maximum swelling pressure. Apart from the initial dry density and the initial water con-
414 tent, the β^* parameter is predominantly controlled by the mass fraction of expansive minerals
415 in the material. This finding is consistent, as EDD might increase with a higher mass fraction
416 of expansive mineral phases at the same dry density. Table 4 gives information about the dif-
417 ferent values of $\sigma_{s, min}$ and β^* .

418 COX_c, the grain- and powder-mixtures were characterized by initial suctions of 1.5 MPa,
419 2.9 MPa and 4.3 MPa, respectively, when the samples were compacted to the maximum dry

420 density at their individual water content by using modified compaction energy. These initial
421 suctions suggest that osmotic swelling might more contribute to the development of swelling
422 pressure under constant-volume conditions than crystalline swelling. As the magnitude of os-
423 motic swelling is susceptible to the saturating solution chemistry, particularly the cations in
424 solution and the ionic strength, the swelling pressures of COX_c and the mixtures were expected
425 to be affected by the employed solution. Interestingly, such an impact was observed only in the
426 case of COX_c whereas both mixtures hardly reacted to the different solutions. The higher sus-
427 ceptibility of COX_c cannot be reasonably explained yet, thus demanding more investigations.

428 6.4 Combined impact of solution chemistry and EDD

429 Comparable to this study, some studies also emphasized the impact of variations in the
430 ionic strength of solutions on the swelling pressure of different bentonites that were compacted
431 to different dry densities (Pusch, 1980; Karnland, 1997; Dixon, 2000; Pusch, 2001; Castellanos
432 et al., 2008; Komine et al., 2009; Xiang et al., 2019). Generally, the impact of the ion concen-
433 tration is more pronounced in the case of less compacted bentonites. The observed effect van-
434 ishes as the dry density and montmorillonite content increase.

435 Conversely, the different saturating solutions had a minor impact on the maximum swell-
436 ing pressure of the grain- and powder-mixtures, even when the samples were compacted to
437 lower values of EDD. This finding can be deduced from $\sigma_{s, min}$ and β^* parameters in Figure 9 a
438 and b, despite the grain-mixture saturated with ABSS exhibited a greater deviation of those
439 parameters. Most probably, the low concentration of cations in solution caused an only partial
440 exchange of cations hardly affecting the thickness of diffuse double layers and in turn the max-
441 imum swelling pressure of the grain- and powder-mixtures.

442 7 Conclusions

443 The current laboratory experimental program assessed the impact of partly replacing
444 crushed COX-claystone (COX_c) with MX80-bentonite on the compaction and on the swelling
445 behavior of mixtures that could potentially be employed to backfill drifts and shafts of a future
446 repository for nuclear waste in deep sedimentary rock formations. Complementary experiments
447 investigated the impact of variations in the dry density and saturating solution chemistry on the
448 evolution of the swelling pressure. The reference concept envisages the employment of con-
449 ventional compaction techniques to install the backfill directly inside the drifts and shafts. The
450 considered backfill materials are composed of 70 % crushed COX-claystone (COX_c) and 30 %
451 MX80-bentonite grains or powder in wet mass. COX_c served as a reference material to identify
452 the impact of the material replacement. Evolving swelling pressures were determined by means
453 of the constant-volume method. The employed samples were then prepared to maximum and
454 reduced dry densities at optimum water contents, which were obtained in modified Proctor tests.
455 The samples were saturated with three solutions, greatly varying in pH values and ionic
456 strengths. The following conclusions can be drawn from the laboratory experimental program:

- 457 1) The replacement of 30% COX_c by either MX80-bentonite grains or powder caused a shift
458 in the maximum dry density to lower values and of the optimum water content to higher
459 values, regardless of the applied compaction energy. Compared to the grain-mixture, the
460 powder-mixture exhibited a higher maximum dry density at a lower initial water content
461 when compacting using the same energy. This finding was attributed to an optimized
462 particle packing caused by a higher amount of fines. The maximum swelling pressure of
463 both mixtures was higher than that of COX_c, despite the lower maximum dry density.
464 Generally, these finding were in accordance with the literature, as the amount of expan-
465 sive minerals phases in the mixtures was higher.

466 2) The swelling pressure of the claystone/ bentonite mixtures was identified as being hardly
467 affected by the saturating solution chemistry, when compacting both mixtures to their
468 maximum dry densities at optimum water contents. This might be caused by the low ionic
469 strength of the employed solutions. The swelling pressure of COX_c seemed to be more
470 susceptible to the saturating solution chemistry. More experiments are required to ade-
471 quately explain this point. Generally applicable, expansive mineral dry density (EDD)
472 improved the comparability of the impact of densification on the swelling pressure of
473 materials that contain fractions of expansive mineral phases. Its introduction was claimed
474 by the considerable contribution of expansive mineral phases in COX_c to material swell-
475 ing. The exponential relationship of EDD and the maximum swelling pressure was iden-
476 tified as being unique in the cases of every bentonite and its mixtures.

477 3) In the case of the grain-and powder-mixture, the different saturating solutions had a minor
478 impact on the maximum swelling pressure of the grain- and powder-mixtures, even when
479 the samples were compacted to lower values of EDD. This finding can be predominantly
480 attributed to the low concentration of cations in solution and the low ionic strength of the
481 employed saturating solutions.

482 It is recommended that MX80-bentonite powder-based mixtures are favored over grain-
483 mixtures if employing conventional compaction techniques to install backfill in drifts and
484 shafts, as higher short-term swelling pressures can be attained. It became evident that varying
485 dry densities affect the material performance of the claystone/ bentonite mixtures more signif-
486 icantly than potential environmental conditions. Thus, high demands must be made on the qual-
487 ity management during backfill installation. Generally, this study improved the knowledge
488 about mixtures of the materials each containing expansive mineral phases in terms of their com-
489 paction and swelling behavior. Future studies will assess the long-term evolution of the material

490 behavior of grain- and powder-mixtures, especially the swelling pressure and hydraulic con-
491 ductivity. It is also of interest to investigate the material behaviors under varying degrees of
492 saturation.

493 Acknowledgement

494 The authors gratefully thank Dr. G. Armand, Dr. N. Michau and Dr. J. Zghondi of AN-
495 DRA for fruitful discussions. The authors also wish to thank the editor and the reviewers for
496 helpful comments on the manuscript.

497 Funding

498 This research did not receive any specific grant from funding agencies in the public, com-
499 mercial, or not-for-profit sectors.

500 **References**

- 501 AFNOR, 1991. Soils: Investigation and testing: Determination of particle density - Pycnome-
502 ter method. Association Francaise de Normalisation (AFNOR).
- 503 AFNOR, 1993. Soils: Investigation and testing: Determination of Atterberg's limits -Liquid
504 limit test using Casagrande apparatus - Plastic limit test on rolled thread. Association
505 Francaise de Normalisation (AFNOR).
- 506 AFNOR, 2014. Soils: Investigation and testing: Determination of the compaction reference
507 values of a soil type - Standard Proctor Test - Modified Proctor Test. Association Fran-
508 caise de Normalisation (AFNOR).
- 509 Agus, S.S., Schanz, T., 2008. A method for predicting swelling pressure of compacted ben-
510 tonites. *Acta Geotech.* 3, 125–137. 10.1007/s11440-008-0057-0.
- 511 Alonso, E.E., Gens, A., Whight, D.W., 1987. General Report, in: Groundwater effects in ge-
512 otechnical engineering. Ninth european conference on soil mechanics and foundation en-
513 gineering, Dublin. 31.08. - 03.09. A. A. Balkema, Rotterdam, Brookfield, pp. 1087–1146.
- 514 Andra, 2005. Dossier 2005 Argile - Synthesis: Evaluation of the feasibility of a geological re-
515 pository in an argillaceous formation (Meuse/ Haute-Marne Site). French National Radio-
516 active Waste Management Agency, Chatenay-Malabry CEDEX, 241 pp. Accessed 22 No-
517 vember 2018.
- 518 Baille, W., Tripathy, S., Schanz, T., 2010. Swelling pressures and one-dimensional compress-
519 ibility behaviour of bentonite at large pressures. *Applied Clay Science* 48, 324–333.
520 10.1016/j.clay.2010.01.002.
- 521 Bolt, G.H., 1956. Physico-chemical analysis of the compressibility of pure clays. *Géotech-*
522 *nique* 6, 86–93.

523 Bradbury, M.H., Baeyens, B., 2003. Porewater chemistry in compacted re-saturated MX-80
524 bentonite. *Journal of Contaminant Hydrology* 61, 329–338. 10.1016/S0169-
525 7722(02)00125-0.

526 Bucher, F., Jedelhauser, P., 1985. Verdichtungsversuche an Quarzsand-Bentonit-Gemischen.
527 Technischer Bericht 85-52. National Cooperative for the Disposal of Radioactive Waste,
528 Zuerich, 25 pp. Accessed 25 February 2019.

529 Castellanos, E., Villar, M.V., Romero, E., Lloret, A., Gens, A., 2008. Chemical impact on the
530 hydro-mechanical behaviour of high-density FEBEX bentonite. *Physics and Chemistry of
531 the Earth, Parts A/B/C* 33, S516-S526. 10.1016/j.pce.2008.10.056.

532 Chen, F.H., 1988. *Foundations on expansive soils*. Elsevier science pub, Amsterdam, New
533 York, 1463 pp.

534 Conil, N., Talandier, J., Djizanne, H., La Vaissière, R. de, Righini-Waz, C., Auvray, C., Mor-
535 lot, C., Armand, G., 2018. How rock samples can be representative of in situ condition: A
536 case study of Callovo-Oxfordian claystones. *Journal of Rock Mechanics and Geotechnical
537 Engineering* 10, 613–623. 10.1016/j.jrmge.2018.02.004.

538 Cuisinier, O., Deneele, D., Masrouri, F., 2009. Shear strength behaviour of compacted clayey
539 soils percolated with an alkaline solution. *Engineering Geology* 108, 177–188.
540 10.1016/j.enggeo.2009.07.012.

541 Cuisinier, O., Deneele, D., Masrouri, F., Abdallah, A., Conil, N., 2014. Impact of high-pH
542 fluid circulation on long term hydromechanical behaviour and microstructure of com-
543 pacted clay from the laboratory of Meuse-Haute Marne (France). *Applied Clay Science*
544 88-89, 1–9. 10.1016/j.clay.2013.12.008.

545 Delage, P., Marcial, D., Cui, Y.J., Ruiz, X., 2006. Ageing effects in compacted bentonite: A
546 microstructure approach. *Géotechnique* 56, 291–304.

547 Dixon, D.A., 2000. Porewater salinity and the development of swelling pressure in bentonite-
548 based buffer and backfill materials. POSIVA 2000-04. POSIVA Oy, Helsinki, 51 pp. Ac-
549 cessed 13 November 2019.

550 Dixon, D.A., Gray, M.N., Thomas, A.W., 1985. A study of the compaction properties of po-
551 tential clay—sand buffer mixtures for use in nuclear fuel waste disposal. *Engineering Ge-*
552 *ology* 21, 247–255. 10.1016/0013-7952(85)90015-8.

553 Gens, A., Alonso, E.E., 1992. A framework for the behaviour of unsaturated expansive clays.
554 *Can. Geotech. J.* 29, 1013–1032. 10.1139/t92-120.

555 Gunnarson, D., Börgesson, L., Hökmark, H., Johannesson, L.-E., Sandén, T., 2001. Äspö
556 Hard Rock Laboratory: Installation of the Backfill and Plug test. *International Progress*
557 *Report 01-17*. Swedish Nuclear Fuel and Waste Management Co, Stockholm, 236 pp. Ac-
558 cessed 20 November 2018.

559 Herbert, H.-J., Kasbohm, J., Moog, H.C., Henning, K.-H., 2004. Long-term behaviour of the
560 Wyoming bentonite MX-80 in high saline solutions. *Applied Clay Science* 26, 275–291.
561 10.1016/j.clay.2003.12.028.

562 ISO, 2009. Particle size analysis: Laser diffraction methods.

563 Johannesson, L.-E., 2014. Prototype Repository: Measurements of water content and density
564 of the retrieved buffer material from deposition hole 5 and 6 and the backfill in the outer
565 section of the Prototype Repository. P-13-14. Swedish Nuclear Fuel and Waste Manage-
566 ment Co, Stockholm, 180 pp. Accessed 8 February 2019.

567 Karnland, O., 1997. Bentonite swelling pressure in strong NaCl solutions – Correlation be-
568 tween model calculations and experimentally determined data. *Technical Report 97-31*.
569 Swedish Nuclear Fuel and Waste Management Co, Stockholm, 40 pp. Accessed 21 No-
570 vember 2018.

571 Karnland, O., Olsson, S., Nilsson, U., Sellin, P., 2007. Experimentally determined swelling
572 pressures and geochemical interactions of compacted Wyoming bentonite with highly al-
573 kaline solutions. *Physics and Chemistry of the Earth, Parts A/B/C* 32, 275–286.
574 10.1016/j.pce.2006.01.012.

575 Keto, P., Kuula-Vaeisaenen, P., Ruuskanen, J., 2006. Effect of Material Parameters on the
576 Compactibility of Backfill Materials. Working Report 2006-34. POSIVA Oy, Olkiluoto.

577 Komine, H., Ogata, N., 1999. Experimental study on swelling characteristics of sand-benton-
578 ite mixture for nuclear waste disposal. *Soils and Foundation* 39, 83–97.

579 Komine, H., Yasuhara, K., Murakami, S., 2009. Swelling characteristics of bentonites in arti-
580 ficial seawater. *Canadian Geotechnical Journal* 46, 177–189. 10.1139/T08-120.

581 Lloret, A., Villar, M.V., Sanchez, M., Gens, A., Pintado, X., Alonso, E.E., 2003. Mechanical
582 behaviour of heavily compacted bentonite under high suction changes. *Géotechnique* 53,
583 27–40. 10.1680/geot.53.1.27.37258.

584 Madsen, F.T., Müller-Vonmoos, M., 1989. The swelling behaviour of clays. *Applied Clay*
585 *Science* 4, 143–156. 10.1016/0169-1317(89)90005-7.

586 Mitchell, J.K., Soga, K., 2005. *Fundamentals of soil behavior*, 3rd ed. Wiley, Hoboken, N.J.,
587 Chichester.

588 Müller-Vonmoos, M., Kahr, G., 1983. Mineralogische Untersuchungen von Wyoming-
589 Bentonit MX-80 und Montigel. Technical Report 83-12. National Cooperative for the Dis-
590 posal of Radioactive Waste, Zuerich, 37 pp. Accessed 17 January 2019.

591 Pusch, R., 1980. Swelling pressure of highly compacted bentonite. Technical Report 80-13.
592 Swedish Nuclear Fuel and Waste Management Co, Stockholm, 35 pp. Accessed 23 No-
593 vember 2018.

594 Pusch, R., 1992. Use of bentonite for isolation of radioactive waste products. *Clay miner.* 27,
595 353–361. 10.1180/claymin.1992.027.3.08.

596 Pusch, R., 1995. Consequences of using crushed crystalline rock as ballast in KBS-3 tunnels
597 instead of rounded quartz particles. Technical Report 95-14. Swedish Nuclear Fuel and
598 Waste Management Co, Stockholm, 51 pp. Accessed 26 February 2019.

599 Pusch, R., 2001. Experimental study of the effect of high porewater salinity on the physical
600 properties of a natural smectitic clay. Technical Report 01-07. Swedish Nuclear Fuel and
601 Waste Management Co, Stockholm, 32 pp. Accessed 21 November 2018.

602 Pusch, R., Yong, R., 2003. Water saturation and retention of hydrophilic clay buffer—micro-
603 structural aspects. *Applied Clay Science* 23, 61–68. 10.1016/S0169-1317(03)00087-5.

604 Pusch, R., Zwahr, H., Gerber, R., Schomburg, J., 2003. Interaction of cement and smectitic
605 clay—theory and practice. *Applied Clay Science* 23, 203–210. 10.1016/S0169-
606 1317(03)00104-2.

607 Robinet, J.-C., Sardini, P., Coelho, D., Parneix, J.-C., Prêt, D., Sammartino, S., Boller, E.,
608 Altmann, S., 2012. Effects of mineral distribution at mesoscopic scale on solute diffusion
609 in a clay-rich rock: Example of the Callovo-Oxfordian mudstone (Bure, France). *Water
610 Resources Research* 48, 819. 10.1029/2011WR011352.

611 Schanz, T., Tripathy, S., 2009. Swelling pressure of a divalent-rich bentonite: Diffuse double-
612 layer theory revisited. *Water Resources Research* 45, 1752. 10.1029/2007WR006495.

613 Sridharan, A., Choudhury, D., 2002. Swelling pressure of sodium montmorillonites. *Géotech-
614 nique* 52, 459–462. 10.1680/geot.2002.52.6.459.

615 Sridharan, A., Rao, A.S., Sivapullaiah, P.V., 1986. Swelling Pressure of Clays. *Geotechnical
616 Testing Journal* 9, 24–33. 10.1520/GTJ10608J.

617 Tang, C.S., Tang, A.M., Cui, Y.J., Delage, P., Schroeder, C., Laure, E. de, 2011a. Investigat-
618 ing the swelling pressure of compacted crushed-Calovo-Oxfordian claystone. *Physics and
619 Chemistry of the Earth, Parts A/B/C* 36, 1857–1866. 10.1016/j.pce.2011.10.001.

620 Tang, C.S., Tang, A.M., Cui, Y.J., Delage, P., Schroeder, C., Shi, B., 2011b. A study of the
621 hydro-mechanical behaviour of compacted crushed argillite. *Engineering Geology* 118,
622 93–103. 10.1016/j.enggeo.2011.01.004.

623 Tang, C.S., Tang, A.M., Cui, Y.J., Delage, P., Shi, B., 2010. The coupled hydro-mechanical
624 behaviours of compacted crushed Callovo-Oxfordian argillite. *Journal of Rock Mechanics*
625 *and Geotechnical Engineering*, 86–90.

626 Tombácz, E., Szekeres, M., 2004. Colloidal behavior of aqueous montmorillonite suspen-
627 sions: the specific role of pH in the presence of indifferent electrolytes. *Applied Clay Sci-*
628 *ence* 27, 75–94. 10.1016/j.clay.2004.01.001.

629 Tombácz, E., Szekeres, M., 2006. Surface charge heterogeneity of kaolinite in aqueous sus-
630 pension in comparison with montmorillonite. *Applied Clay Science* 34, 105–124.
631 10.1016/j.clay.2006.05.009.

632 van Olphen, H., 1977. *An introduction to clay colloid chemistry: For clay technologists, geol-*
633 *ogists, and soil scientists*, 2nd ed. Wiley, New York (N.Y.), 1318 pp.

634 Villar, M.V., Rivas, P., 1994. Hydraulic properties of montmorillonite-quartz and saponite-
635 quartz mixtures. *Applied Clay Science* 9, 1–9. 10.1016/0169-1317(94)90011-6.

636 Wang, Q., Cui, Y.J., Tang, A.M., Delage, P., Gatmiri, B., Ye, W.M., 2014. Long-term effect
637 of water chemistry on the swelling pressure of a bentonite-based material. *Applied Clay*
638 *Science* 87, 157–162. 10.1016/j.clay.2013.10.025.

639 Wang, Q., Tang, A.M., Cui, Y.J., Delage, P., Gatmiri, B., 2012. Experimental study on the
640 swelling behaviour of bentonite/claystone mixture. *Engineering Geology* 124, 59–66.
641 10.1016/j.enggeo.2011.10.003.

642 Xiang, G., Xu, Y., Yu, F., Fang, Y., Wang, Y., 2019. Prediction of swelling characteristics of
643 compacted GMZ bentonite in salt solution incorporating ion-exchange reactions. *Clays*
644 *Clay Miner.* 67, 163–172. 10.1007/s42860-019-00014-3.

- 645 Yong, R.N., 1999. Soil suction and soil-water potentials in swelling clays in engineered clay
646 barriers. *Engineering Geology* 54, 3–13. 10.1016/S0013-7952(99)00056-3.
- 647 Zeng, Z., Cui, Y.J., Zhang, F., Conil, N., Talandier, J., 2019. Investigation of swelling pres-
648 sure of bentonite/claystone mixture in the full range of bentonite fraction. *Applied Clay*
649 *Science* 178, 105137. 10.1016/j.clay.2019.105137.

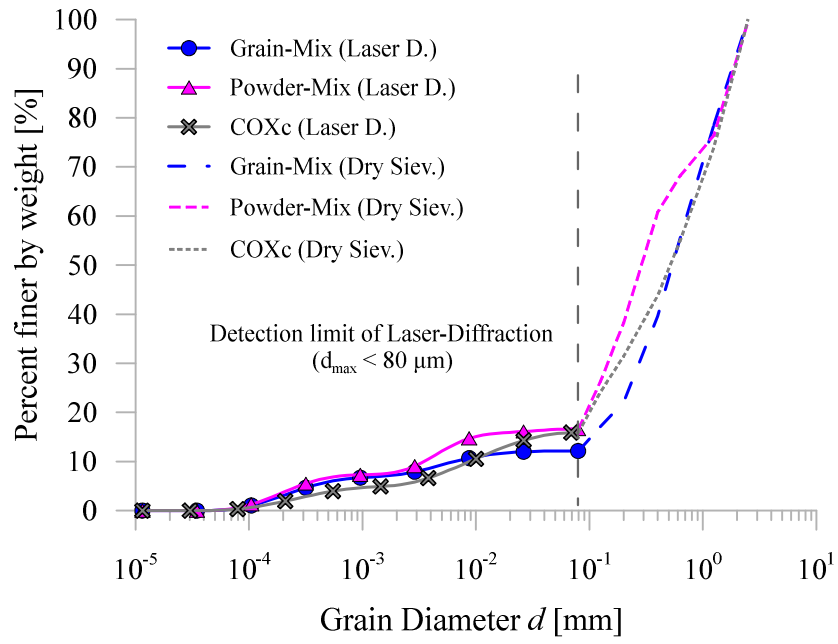


Figure 1: Grain size distribution curves of COXc, grain- and powder-mixtures obtained by dry sieving and laser diffractometry

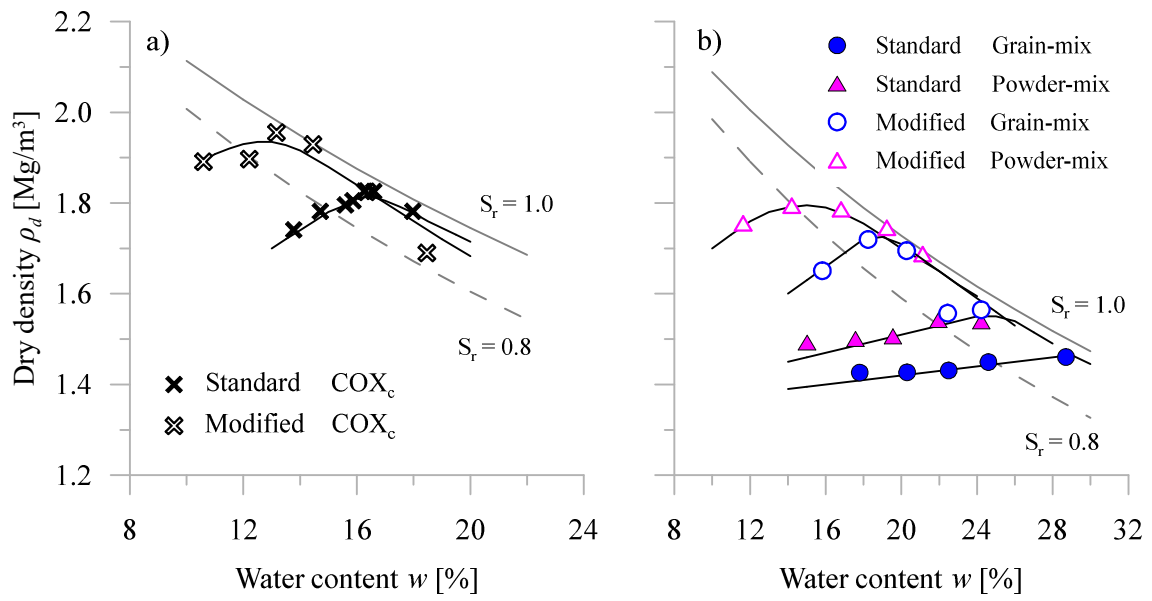


Figure 2: a) Results of the standard and modified Proctor tests performed on COXc, b) Results of the standard and modified Proctor tests performed on the grain- and powder-mixtures

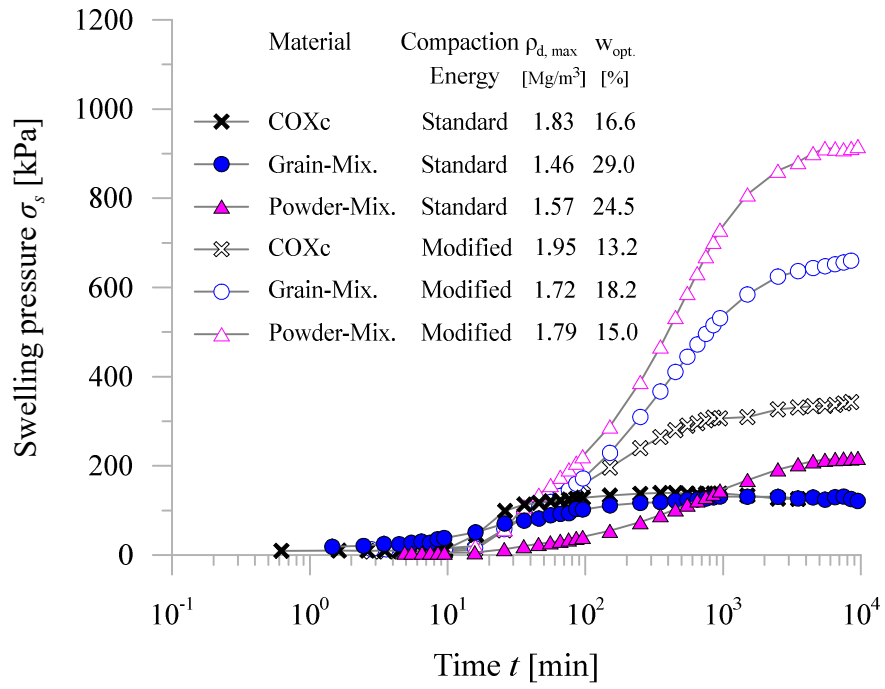


Figure 3: Evolution of swelling pressure of COXc, grain- and powder-mixture compacted to their individual maximum dry densities at optimum water contents and saturated with demineralised/deaired water (DW)

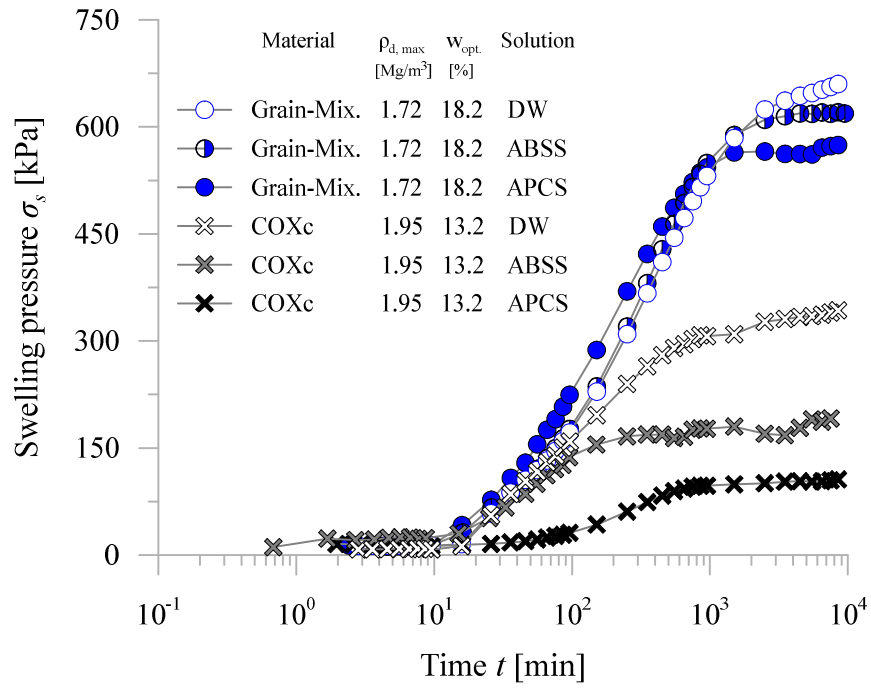


Figure 4: Evolution of swelling pressure of COXc and the grain-mixture compacted to the individual maximum dry densities at optimum water contents and saturated with demineralised/deaired water (DW), artificial Bure site solution (ABSS) and artificial Portland cement solution (APCS))

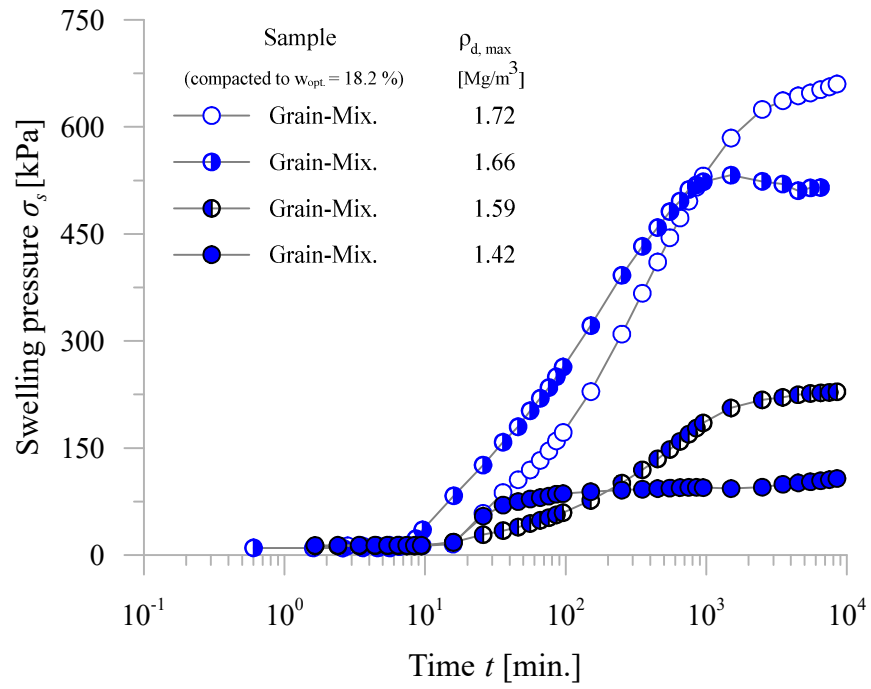


Figure 5: Evolution of swelling pressure of the grain-mixture compacted to 1) maximum dry density, 2) maximum dry density reduced by 3.5%, 3) maximum dry density reduced by 7.5%, and 4) maximum dry density reduced by 17.5% at optimum water content and saturated with deaired/demineralised water (DW)

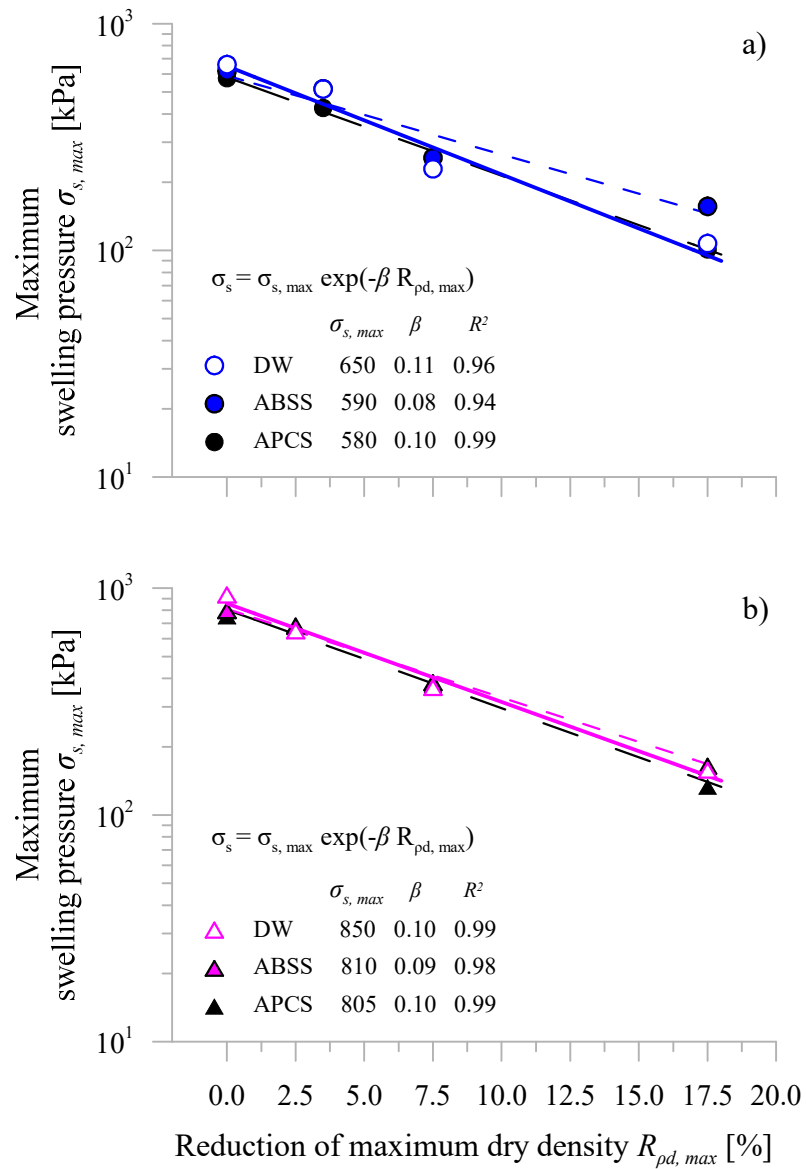


Figure 6: Depiction of the exponential relation between the reduction of initial dry density and the maximum swelling pressure, including the impact of the saturating solution chemistry: a) Relation of grain-mixture, b) Relation of powder-mixture

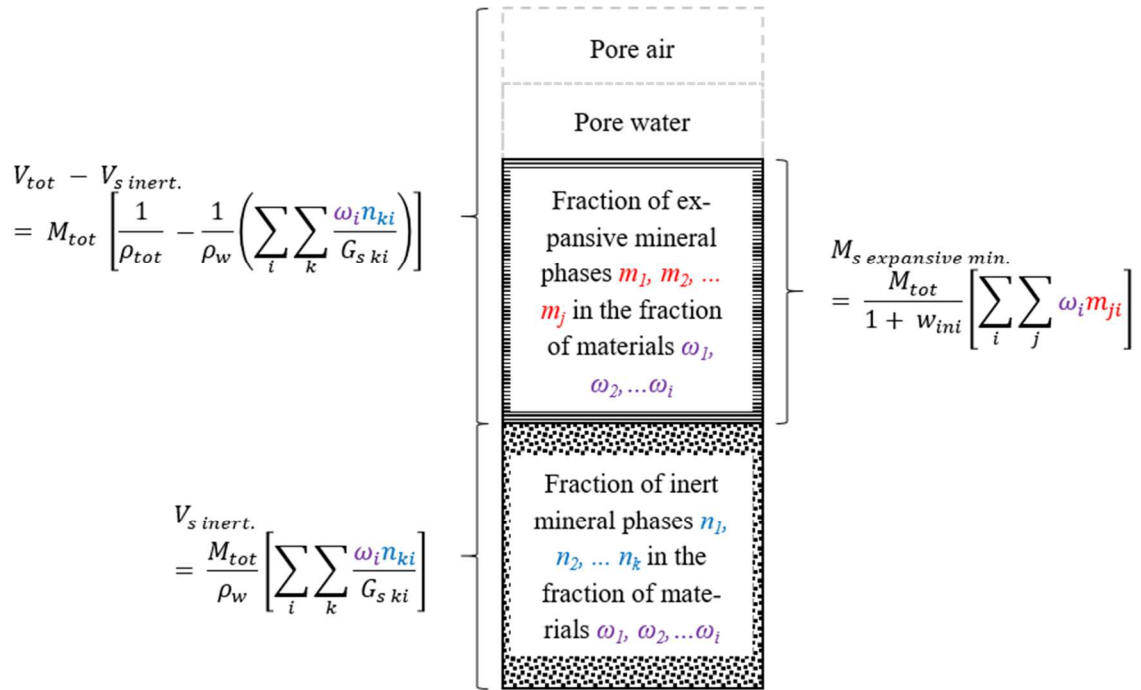


Figure 7: Defined four phases of a mixture composed of different expansive clays

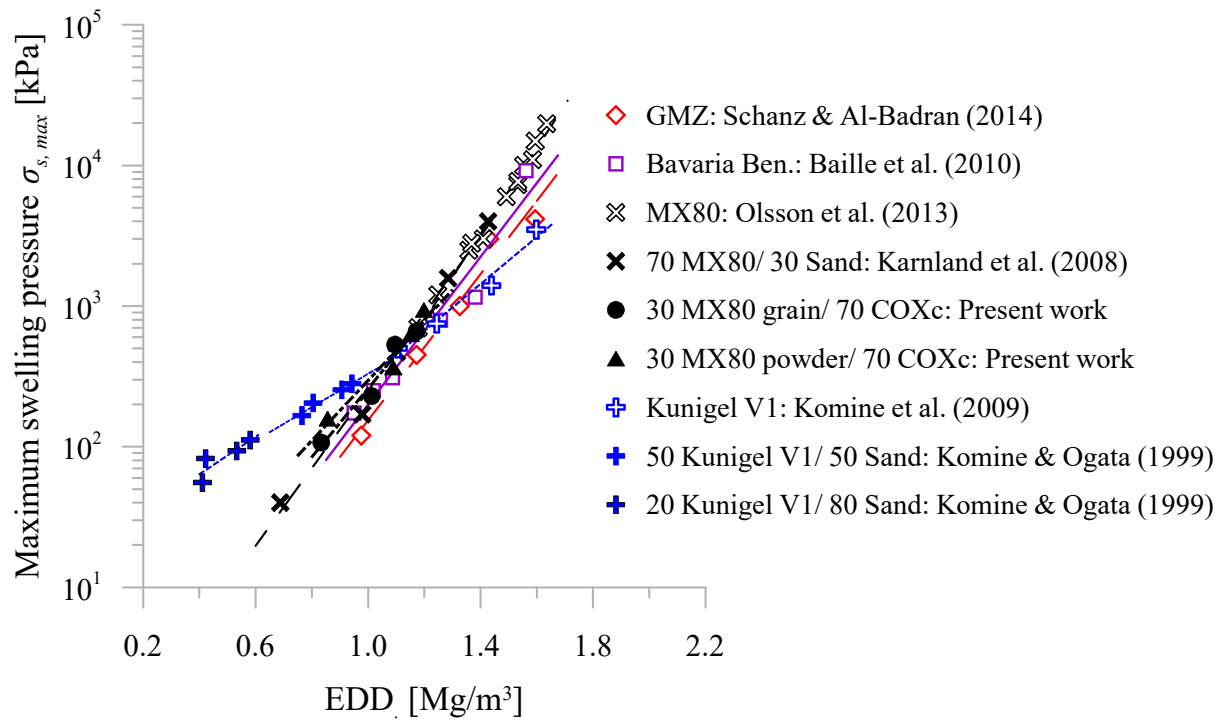


Figure 8: Exponential relationship of EDD and the maximum swelling pressure including results of various expansive clays and their mixtures with varying amounts of non-expansive material taken from the literature

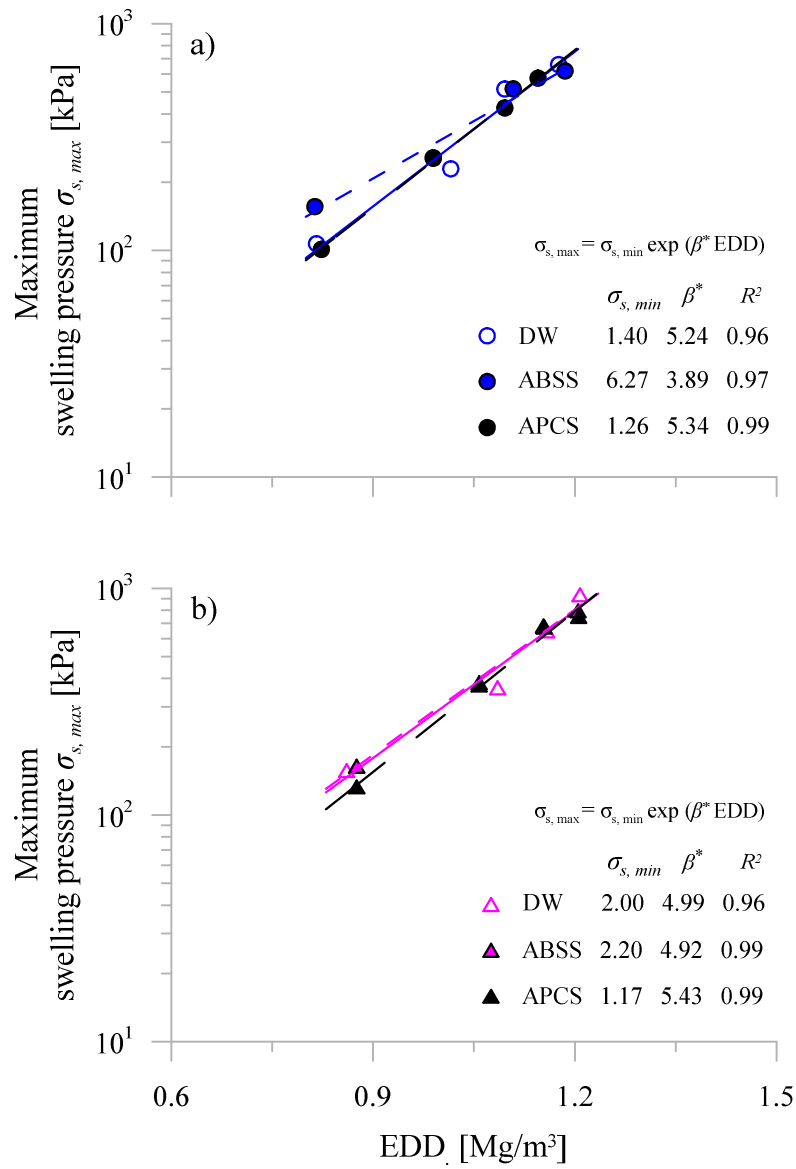


Figure 9: Exponential relation of EDD and maximum swelling pressure in the case of the a) grain-mixture and b) the powder-mixture (saturated with deaired/demineralised water (DW), artificial Bure site solution (ABSS) and artificial Portland cement solution (APCS))

Mineral		Müller-Vonmoos and Kahr (1983)	Herbert et al. (2004)	Karnland et al. (2007)
Carbonate	[%]	1	< 2	1
Cristobalite	[%]	-	< 2	3
Feldspar	[%]	7	2	7
Kaolinite	[%]	< 1	-	-
Mica	[%]	< 1	-	1
Montmorillonite	[%]	75	90	83
Quartz	[%]	15	4	5
Pyrite	[%]	> 1	> 1	-

1 Table 1: Mineralogical composition of MX80-bentonite taken from literature

Material	Physical properties					
	Natural water content w [%]	Specific gravity G _s [-]	Liquid limit LL [%]	Plastic limit PL [%]	10 %-Passing D ₁₀ [mm]	60 %-Passing D ₆₀ [mm]
COX _c	5.4	2.68	37.3	24.9	0.01	0.8
MX80 ^{a, b}	-	2.65 - 2.88	420.0 - 520.0	38.0 - 65.0	-	-
Grain mix.	6.4	2.64	112.5	34.7	0.008	0.8
Powd. mix.	6.4	2.64	112.5	34.7	0.004	0.2

^a : Delage et al. (2006)

^b : Komine et al. (2009)

1 Table 1: Determined physical properties of COX_c, MX80-bentonite, grain- and powder-mixture

Compound/ Main ion species	Artificial Bure Site Solution (ABSS)		Artificial Portland Cement Solution (APCS)
		c (Compound) [mmol/l]	c (Compound) [mmol/l]
NaCl		33.4	22.1
NaHCO ₃		1.5	-
Na ₂ SO ₄		4.9	-
KCl		0.5	8.0
Ca(OH) ₂		-	19.0
CaSO ₄ *2H ₂ O		4.6	-
CaCl ₂ *2H ₂ O		0.7	-
MgSO ₄ *7H ₂ O		8.5	-
I	[mmol/l]	105.0	87.0
pH	[-]	7.8	12.4

c (Compound): Molar concentration of the compound

1 Table 3: Compounds and characteristics of solutions being employed

Reference	Material	$\sum \sum f_i x_{ji}$	$\sigma_{s, min}$	β^*	R^2
		[-]	[kPa]	[-]	[-]
Schanz and Al-Badran (2014)	GMZ01 bentonite	0.75	0.39	5.99	0.971
Baille et al. (2010)	Bavaria bentonite	0.78	0.47	6.05	0.947
Olsson et al. (2013)	MX80 bentonite	0.83	0.15	7.59	0.907
Karland et al. (2007)	70 % MX80/ 30 % Sand	0.58	0.42	6.78	0.992
Komine et al. (2009)	Kunigel V1 bentonite	0.57	6.60	3.85	0.975
Komine and Ogata (1999)	50 % Kunigel/ 50 % Sand	0.17	32.00	1.97	0.617
Komine and Ogata (1999)	20 % Kunigel/ 80 % Sand	0.11	18.68	2.58	0.751
Present work: Grain-mix.	30 % MX80 gr./ 70 COX _c	0.35	1.40	5.24	0.962
Present work: Powder-mix.	30 % MX80 po./ 70 COX _c	0.35	2.00	4.99	0.963

$\sum \sum f_i x_{ji}$: Accumulated mass fraction of expansive minerals (in the mixture)

1 Table 4: Material parameters obtained by correlation of experiment and literature data